# NASA TECHNICAL MEMORANDUM

NASA TM X-71719

NASA TM X-71719

(NASA-TM-X-71719) A COMPRESSOR DESIGNED FOR THE ENERGY RESEARCH AND DEVELOPMENT AGENCY AUTOMOTIVE GAS TURBINE PROGRAM (NASA) 32 p HC $3.75 CSCL 21E

N75-24116

Unclas
G3/44 22206

# A COMPRESSOR DESIGNED FOR THE ENERGY RESEARCH AND DEVELOPMENT AGENCY AUTOMOTIVE GAS TURBINE PROGRAM

by Michael R. Galvas
Lewis Research Center
U.S. Army Air Mobility R&D Laboratory
Cleveland, Ohio 44135

May 1975

## ABSTRACT

A centrifugal compressor was designed for a gas turbine powered automobile as part of the Energy Research and Development Agency program to demonstrate emissions characteristics that meet 1978 standards with fuel economy and acceleration which are competitive with conventionally powered vehicles. A backswept impeller was designed for the compressor in order to attain the efficiency goal and range required for the objectives of this program. Details of the design and method of flow analysis of the compressor are presented herein.

E-8365

## SUMMARY

A centrifugal compressor was designed for a gas turbine powered automobile as part of a program to demonstrate emissions characteristics that meet 1978 standards with fuel economy and acceleration which are competitive with conventionally powered vehicles. The selected design point characteristics of the compressor are: mass flow rate, 0.59 kg/sec; rotative speed, 58,500 rpm; total pressure ratio, 4.08; and total efficiency, .775. A backswept impeller was designed for the compressor in order to attain the efficiency and operating range goals of this program. Design inlet Mach number for the diffuser was chosen to be 0.85 for additional operating range over that obtainable with inlet Mach numbers closer to sonic. Downstream of the diffuser, a constant depth duct turns the flow from radial to axial. In the axial section, constant height vanes remove the swirl before the flow enters the regenerator inlet. Details of the design and analysis of the impeller, diffuser, turning duct, and deswirl vanes are presented herein.

# INTRODUCTION

The Energy Research and Development Agency (ERDA) is conducting a program to demonstrate a gas turbine powered automobile that meets the 1978 Federal Emissions Standards with acceleration characteristics and fuel economy that are competitive with current conventionally powered vehicles. Part of this program involves vehicle and test stand evaluations of an existing sixth generation engine manufactured by the Chrysler Corporation. Another part of the program consists of the design of a new engine to meet the objectives of the program with a significant improvement in vehicle kilometers per liter.

The existing or "baseline" engine delivers 112 KW in a 2000 Kg vehicle. The new or "upgraded" engine will deliver 75 KW in a 1600 Kg vehicle with the capability of power augmentation to 90 KW through the use of variable guide vanes and water injection at the compressor inlet. Improved fuel economy will result from the reduced vehicle weight, reduced power to weight ratio, increased turbine inlet temperature and possible improvements in component efficiencies. The aerodynamic components for the "upgraded" engine have been designed at the Lewis Research Center. These include the compressor, the compressor-drive turbine, the power turbine, the duct between the turbines, and the power turbine exit diffuser. This report presents the details of the aerodynamic design of the "upgraded" compressor.

The design mass flow rate for the "upgraded" compressor was 0.59 kg/sec. Reference 1 along with parametric studies indicates that stage efficiency and flow range can be improved by using a backswept instead

of a radial impeller. Therefore, a backswept configuration was selected for the "upgraded" compressor to help attain the efficiency goal of this program. The "upgraded" compressor design velocity diagrams and overall geometry were selected on the basis of engine response and packaging requirements, stress limitations and stage performance optimization studies.

The following sections discuss the preliminary and detailed design of the compressor together with the methods of calculation and assumptions used in the compressor design. Design point velocity diagrams and state conditions are given for various stations throughout the stage. The velocity diagrams are deduced from the effective flow areas dictated by the assumed loss at the various stations. Blade and vane geometry and surface velocity distributions are given for the impeller, channel diffuser, and deswirl vanes. Also, the wall velocity distributions for the turning duct between the channel diffuser and deswirl vanes are given.

## PRELIMINARY DESIGN

As stated in the INTRODUCTION, the net unaugmented power output was 75 KW. This power level together with the pressure ratio (4.08:1), the compressor turbine inlet temperature (1324 K), estimated component efficiencies and estimated parasitic and leakage losses were used to determine a first estimate of state points and mass flow along the engine flow path using an engine cycle computer program. Using these state points and mass flow, a compressor optimization study was made using the loss model of reference 2 covering a range of rotative speeds from 55,000 rpm to 70,000 rpm and a range of backsweep angles from zero to 45 degrees. A minimum inducer hub diameter of 5.08 cm was also specified to meet a constraint imposed by the starter clutch. Other engine constraints such as gas generator acceleration time and packaging as well as stress limitations were imposed to make the final configuration selection. Similar optimizations studies were executed for the other components. Final estimates were then made for all component efficiencies and other losses and used to make a final engine cycle calculation to obtain the design values of state points and flow rate along the engine flow path.

The compressor design point mass flow is 0.59 kg/sec and the design rotative speed is 58,500 rpm. Rotative speeds up to 30% higher have compressor efficiencies up to one point higher than the selected speed. However, a stress limitation in the compressor turbine precluded the selection of a higher rotative speed. A peak stage efficiency of 0.79 is considered to be achievable for the current

state of the art. Higher efficiencies are quoted in the literature for this pressure ratio and flow rate. However, considering the thickness of the blades and the geometrical compromises required by the method of fabrication, it appears that a peak efficiency of 0.79 is a realistic objective. An additional constraint on the compressor design was that its design point be 2 to 3% from choke for the purpose of improved incidence and additional surge margin at part power operation. This results in a design point efficiency that is about one point below the peak efficiency.

The upgraded compressor has a specific speed of .61. This value is the same as for the baseline compressor. Table I gives a comparison of salient parameters for both compressors. The table shows that a backsweep angle of 30° was selected for the upgraded design. This selection was based on the best overall stage efficiency and flow range. The selection of a backward curved design resulted in increased gas generator acceleration time because of increased rotating inertia. Increased inertia increases fuel consumption because of the nature of the duty cycle for automotive engines. This nullifies some of the benefits from efficiency gains obtained by the use of backward curvature. However, the increase in flow range obtained with backward curvature was sufficient to justify its selection.

Some of the other parameters and geometry that were specified or obtained in the optimization study and stage efficiency calculations are the inducer tip diameter, the number of impeller blades and an associated work factor, the ratio of impeller exit-to-inducer tip relative velocity ratio and the vaneless diffuser radius ratio. An

inducer tip diameter of 8.95 cm was selected which together with the minimum hub diameter of 5.08 cm results in an axial Mach number of 0.382.

Fifteen, seventeen and eighteen blades were assumed in the preliminary design. It is desired to have as few blades as possible to minimize inertia. The associated work factors (ratio of impeller exit absolute tangential velocity-to-impeller exit blade speed) are .7466, .7548 and .7580 respectively. These work factors are consistent with conventional slip criteria. These work factors and the selected rotative speed results in impeller exit tip diameters of 16.76 cm, 16.70 cm and 16.64 cm. It should be noted that the selection of a larger number of blades reduces the tip diameter so that the increase in inertia due to more blades tends to be compensated for by a reduced tip diameter. Eighteen blades were chosen for the final design on the basis of tradeoffs between impeller loadings and inertia.

The impeller exit-to-inducer tip relative velocity ratio was selected to give an impeller exit absolute flow angle of approximately seventy degrees from radial. This was chosen so that during engine accelerations the impeller exit flow angle would not exceed 75 degrees. Design values of absolute flow angle over 70° tend to limit compressor flow range. This results from reduced radial momentum and increased flow path length in the vaneless space.

A vaneless diffuser at the impeller exit with a radius ratio of 1.11 was selected to give a vaned diffuser leading edge Mach number of .85. This selection gives a peak stage efficiency somewhat lower

than the optimum, but provides additional operating range over that obtainable with a higher diffuser leading edge Mach number. The loss in stage performance is attributable to lower overall static pressure recovery in the vaned diffuser caused by increased vaned diffuser inlet blockage.

The estimated design point loss distribution is summarized in Table 2. Other geometry not determined in the preliminary design program were the overall channel diffuser, turning duct, and deswirl vane.

The diffuser geometry was selected as follows: the diffuser inlet radius of 9.22 cm was dictated by the selection of the inlet Mach number. The exit radius of 12.7 cm was selected because of engine packaging requirements. A channel divergence angle of 13 degrees was selected for the design inlet Mach number of 0.85 and the calculated throat aerodynamic blockage of 9.0 percent.

Downstream of the channel diffuser a constant depth turning duct was chosen to guide the swirling flow from radial to axial. The inner radius of the duct was chosen to be twice the depth of the duct. During the preliminary layout it was felt that the desired velocity distributions could be achieved if the inner wall radius-to-duct depth ratio was less than 2.5.

Constant height axial vanes were used to further diffuse the flow before it enters the collector for entry into the regenerator. Axial chord of the vanes was limited to 2.16 cm because of engine packaging constraints.

The final compressor path design velocity diagrams and state conditions are shown in Figure 1. A meridional cross section of the flow path is shown in Figure 2 and salient flow path dimensions are tabulated in Table 3. The detailed design and flow calculations are presented in the following section.

# DETAILED DESIGN

## Impeller

The initial impeller meridional contour was constructed using mathematical curves for the hub and shroud. An initial blade shape was constructed by matching blade angles at the inlet and exit to those required by part-power incidence and blade backsweep with numerically smoothed curves between the endpoints. Near zero incidence from free stream to blade mean camber line along the inducer span was specified at the design point to obtain more favorable incidence and consequently, additional surge margin at part power operation. A meridional plane flow solution was obtained using the computer program of reference 3. Iterations on meridional length, meridional shape, and blade angle distribution were made until the desired incidence and velocity distributions along the blade surfaces were obtained. In the meridional analysis, the primary objectives were to obtain near-uniform loading along the shroud meridional length with most of the diffusion occurring within the inducer. High initial diffusion was considered acceptable because the boundary layer is most able to withstand the adverse pressure gradient without separating. Light diffusion along the shroud downstream of the inducer was used in an attempt to minimize the potential for flow separation, which is most likely to occur first at the shroud section. Velocity peaks and shroud suction surface diffusion were also minimized to promote flow stability.

Detailed blade geometry and flow path information output from the final meridional plane solution were used as input for a blade-

to-blade solution as described in reference 4. The final blade angle distributions for the hub, mean and tip sections are shown in Figure 3, and the blade surface velocity distributions from the blade-to-blade solution for these three sections are shown in Figures 4a, b, and c. Figure 4c shows that near uniform loading was achieved along the shroud meridional length with low diffusion outside the inducer region. The requirements of zero incidence and uniform loading result in some high initial acceleration of the shroud suction surface velocity near the leading edge. Attempts to further load the inducer were considered undesirable because of severe acceleration and subsequent diffusion of the suction surface velocity. The magnitude of suction surface diffusion shown in the figure was considered to be acceptable because tests of impellers in this pressure ratio and flow range, operating at this incidence, indicate penalties of only about one point in efficiency. The three figures also show that other than the inducer there are no severe local velocity gradients that could cause separation.

## Channel Diffuser

The primary considerations in the detailed design of the channel diffuser were incidence for adequate surge margin and throat area required for the design point mass flow. Parallel endwalls downstream of the impeller were used throughout the diffusing system. The wall spacing was equal to the impeller exit blade height plus the axial clearance at the impeller exit. Results of the preliminary design indicated that the absolute flow angle at the channel diffuser leading edge was 70.3 degrees from radial. Four degrees negative

incidence to the channel diffuser mean line setting angle was considered desirable from a surge margin standpoint. This resulted in a vane mean line setting angle of 74.3 degrees from radial. Empirical correlations (reference 5) based on impeller exit absolute Mach number and vaneless diffuser static pressure rise indicated that 9.0 percent aerodynamic blockage could be expected at the channel diffuser inlet. Several diffuser configurations with various numbers of vanes were constructed using this setting angle but it was found that the diffuser would be choked when the anticipated aerodynamic blockage was included in the inviscid flow calculations. In order to provide additional throat area the incidence angle was compromised and the vanes were rotated toward radial. The final diffuser configuration had fourteen vanes with a mean line setting angle of 73.5 degrees from radial. This satisfied the throat area requirement and still provided negative incidence for surge margin. Channel divergence of 13 degrees was selected to give maximum static pressure recovery for the length available. The data of reference 6 for throat aspect ratios of 0.25 were used for the design inlet Mach number and throat blockage in making this selection. Channel divergence angles of 12° to 14° result in maximum static pressure recovery when the diffuser overall length-to-inlet width ratio is optimized. Although this channel diffuser is considerably shorter than optimum because of the engine packaging constraint, 13° divergence was selected in an attempt to maximize static pressure recovery within the available length. A radial plane view of the channel diffuser is shown in Figure 5. The blade-to-blade surface velocity distribution for the channel diffuser

is shown in Figure 6. The figure shows maximum loading just inside the channel diffuser leading edge with progressively decreasing loading along the meridional length.

## Turning Duct

The turning duct geometry is completely specified by two circular arc surfaces of revolution. The inner wall radius is 0.852 cm and the outer wall radius is 1.279 cm. The inlet annulus is located at a radius of 12.7 cm from the axis of rotation. Inlet station conditions are those which correspond to the exit of the channel diffuser. Approximately 37.5 degrees of swirl remains in the flow just inside the channel at the diffuser exit. Rapid expansion, assumed to occur at constant total pressure, around the channel diffuser trailing edges results in an absolute flow angle of about 57° from radial. Angular momentum remains relatively constant throughout the turning duct although some diffusion and reduction of the tangential velocity is achieved through the slight increase in the duct mean streamline radius. The flow solution for the turning duct was computed using the meridional plane analysis of reference 3. The velocity distributions along the hub and shroud are shown in Figure 7.

## Deswirl Vanes

Sixty constant height axial vanes are used to remove the swirl remaining in the flow before it enters the collector for the regenerator inlet. The number of vanes was selected primarily on the basis of solidity. Axial chord was limited to 2.16 cm for engine packaging. Several mean camber line angle distributions investigating various rates of turning were studied in the design. Approximately three

degrees of negative incidence were used to control suction surface diffusion. Eight degrees deviation at the trailing edge resulted in axial flow. The final mean camber line angle distribution, shown in Figure 8, has the maximum curvature just upstream of the mid-axial chord. Past experience indicates that this type of distribution gives favorable results. A .152 cm constant thickness vane was overlaid on this mean camber line. The blade-to-blade surface velocity distribution for the deswirl vanes is shown in Figure 9. The figure shows maximum loading just upstream of the mid-axial chord with rapid suction surface diffusion and light loading near the trailing edge.

## SYMBOLS

| | |
|---|---|
| $m$ | meridional length, cm |
| $M$ | Mach number |
| $p'$ | total pressure, $N/cm^2$ |
| $r$ | radius, cm |
| $R_c$ | total pressure ratio |
| $T'$ | total temperature, K |
| $u$ | blade speed, m/sec |
| $V$ | absolute velocity, m/sec |
| $w$ | mass flow rate, kg/sec |
| $W$ | relative velocity, m/sec |
| $\alpha$ | absolute flow angle, deg from meridional |
| $\beta$ | relative flow angle, deg from meridional |
| $\delta$ | ratio of total pressure to standard sea-level total pressure |
| $\Delta$ | incremental quantity |
| $\eta$ | total efficiency |
| $\theta$ | relative angular coordinate defined in Figure 2 |
| $\theta_i$ | ratio of total temperature to standard sea-level total temperature |

Subscripts:

| | |
|---|---|
| $u$ | tangential direction |
| $m$ | meridional direction |

## REFERENCES

1. Weigel, Carl; Ball, Calvin L.; and Tysl, Edward R.: Overall Performance in Argon of a 16.4-Centimeter (6.44-in.) Sweptback-Bladed Centrifugal Compressor. NASA TM X-2269.

2. Galvas, Michael R.: Fortran Program for Calculating Total-Efficiency-Specific Speed Characteristics of Centrifugal Compressors. NASA TM X-2594, 1972.

3. Katsanis, Theodore; and McNally, William D.: Fortran Program for Calculating Velocities and Streamlines on the Hub-Shroud Mid-Channel Flow Surface of an Axial- or Mixed-Flow Turbomachine. NASA TN D-7343, 1973.

4. Katsanis, Theodore: Fortran Program for Calculating Transonic Velocities on a Blade-to-Blade Stream Surface of a Turbomachine. NASA TN D-5427, 1969.

5. Kenny, D. P.: A Comparison of the Predicted and Measured Performance of High Pressure Ratio Centrifugal Compressor Diffusers. ASME Paper 72-GT-54.

6. Runstadler, Peter W., Jr.: Pressure Recovery Performance of Straight-Channel, Single-Plane Divergence Diffusers at High Mach Numbers. USAAVLABS Technical Report 69-56, 1969.

| TABLE 1 – COMPARISON OF COMPRESSORS | | |
|---|---|---|
| | BASELINE | UPGRADED |
| MASS FLOW RATE $w\sqrt{\theta}/\delta$, kg/sec | 1.03 | 0.61 |
| PRESSURE RATIO | 4.08 | 4.08 |
| ROTATIVE SPEED, rpm | 44610 | 58500 |
| EFFICIENCY, $\eta$ | .777 | .775 |
| IMPELLER BLADING | RADIAL | BACKSWEPT 30° |
| SPECIFIC SPEED | 0.61 | 0.61 |



| TABLE 2 COMPRESSOR LOSS DISTRIBUTION | |
|---|---|
| LOSS GENERATOR | EFFICIENCY DECREMENT, $\Delta\eta$ |
| IMPELLER BLADE LOADING | .059 |
| SKIN FRICTION | .054 |
| DISK FRICTION | .018 |
| IMPELLER DISCHARGE RECIRCULATION | .007 |
| VANELESS DIFFUSER | .044 |
| VANED DIFFUSER | .043 |

| TABLE 3 COMPRESSOR GEOMETRY | |
|---|---|
| INDUCER HUB DIAMETER, cm. | 5.08 |
| INDUCER TIP DIAMETER, cm. | 8.95 |
| INDUCER RADIAL CLEARANCE, cm. | .025 |
| IMPELLER AXIAL LENGTH, cm. | 3.75 |
| IMPELLER EXIT DIAMETER, cm. | 16.64 |
| IMPELLER EXIT BACKSWEEP, deg from radial | 30 |
| IMPELLER EXIT BLADE HEIGHT, cm. | .401 |
| IMPELLER EXIT AXIAL CLEARANCE, cm. | .025 |
| DIFFUSER DEPTH, cm. | .426 |
| DIFFUSER INLET DIAMETER, cm. | 18.43 |
| DIFFUSER EXIT DIAMETER, cm. | 25.40 |
| TURNING DUCT INNER WALL RADIUS, cm. | .852 |
| TURNING DUCT OUTER WALL RADIUS, cm. | 1.279 |
| DESWIRL VANE HEIGHT, cm. | .426 |
| DESWIRL VANE AXIAL CHORD, cm. | 2.16 |

# IMPELLER VELOCITY DIAGRAMS

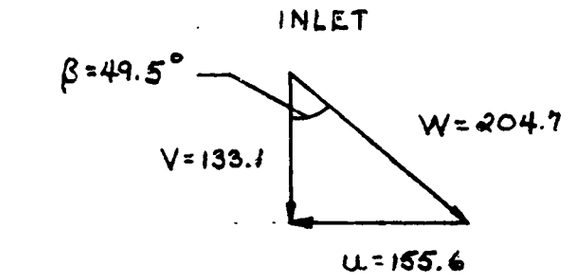


$p' = 9.98$ N/cm²

$T' = 302.8$ K

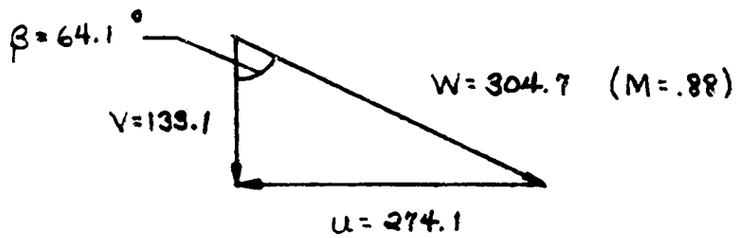


EXIT MEAN

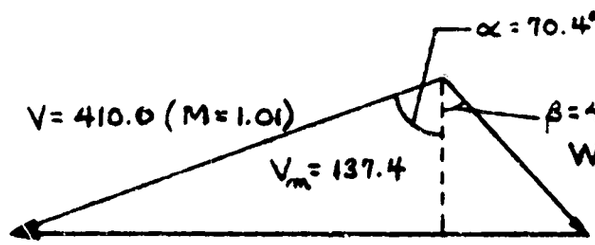


$p' = 46.5$ N/cm²

$T' = 492$ K

FIGURE 1 - DESIGN POINT VELOCITY DIAGRAMS

DIFFUSER VELOCITY DIAGRAMS

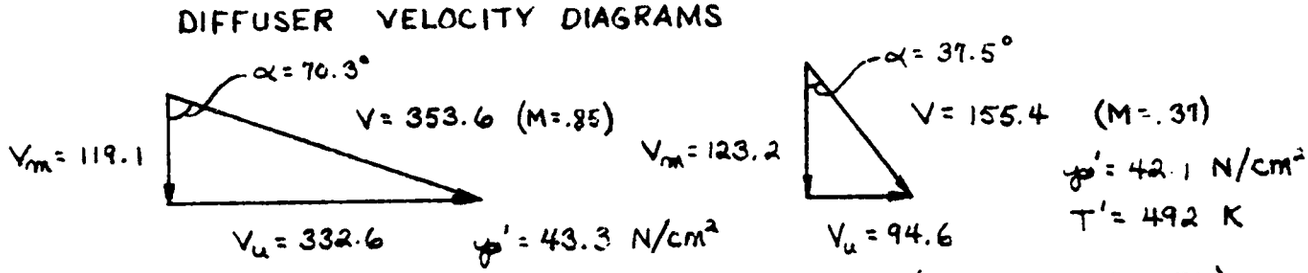


TURNING DUCT VELOCITY DIAGRAMS
MEAN STREAMLINE

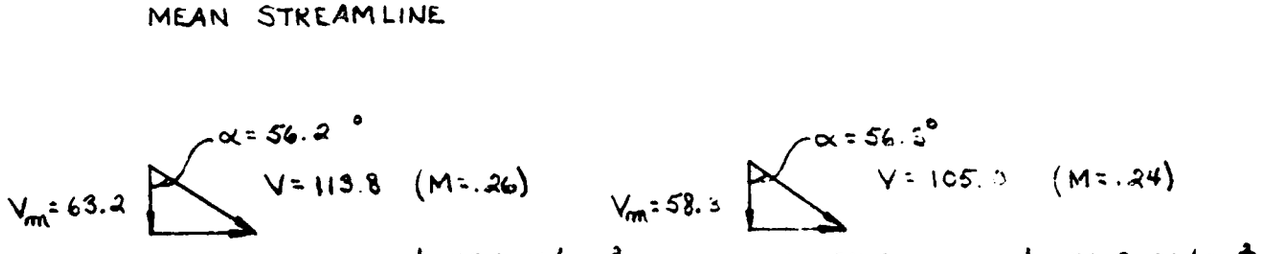


DESWIRL VANE VELOCITY DIAGRAMS
MEAN STREAMLINE

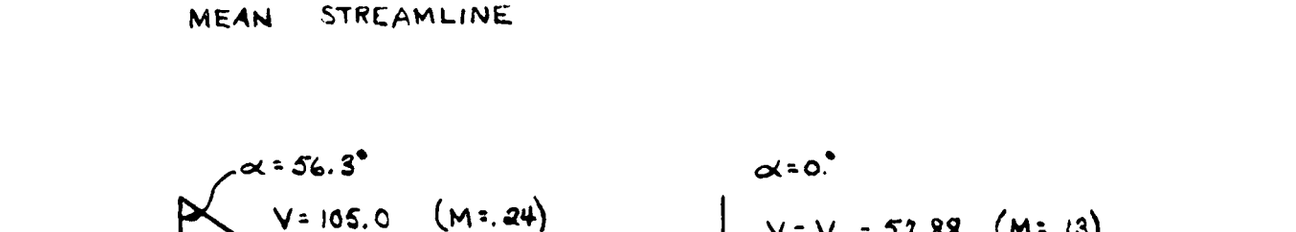


FIGURE 1- DESIGN POINT VELOCITY DIAGRAMS (CONCLUDED)

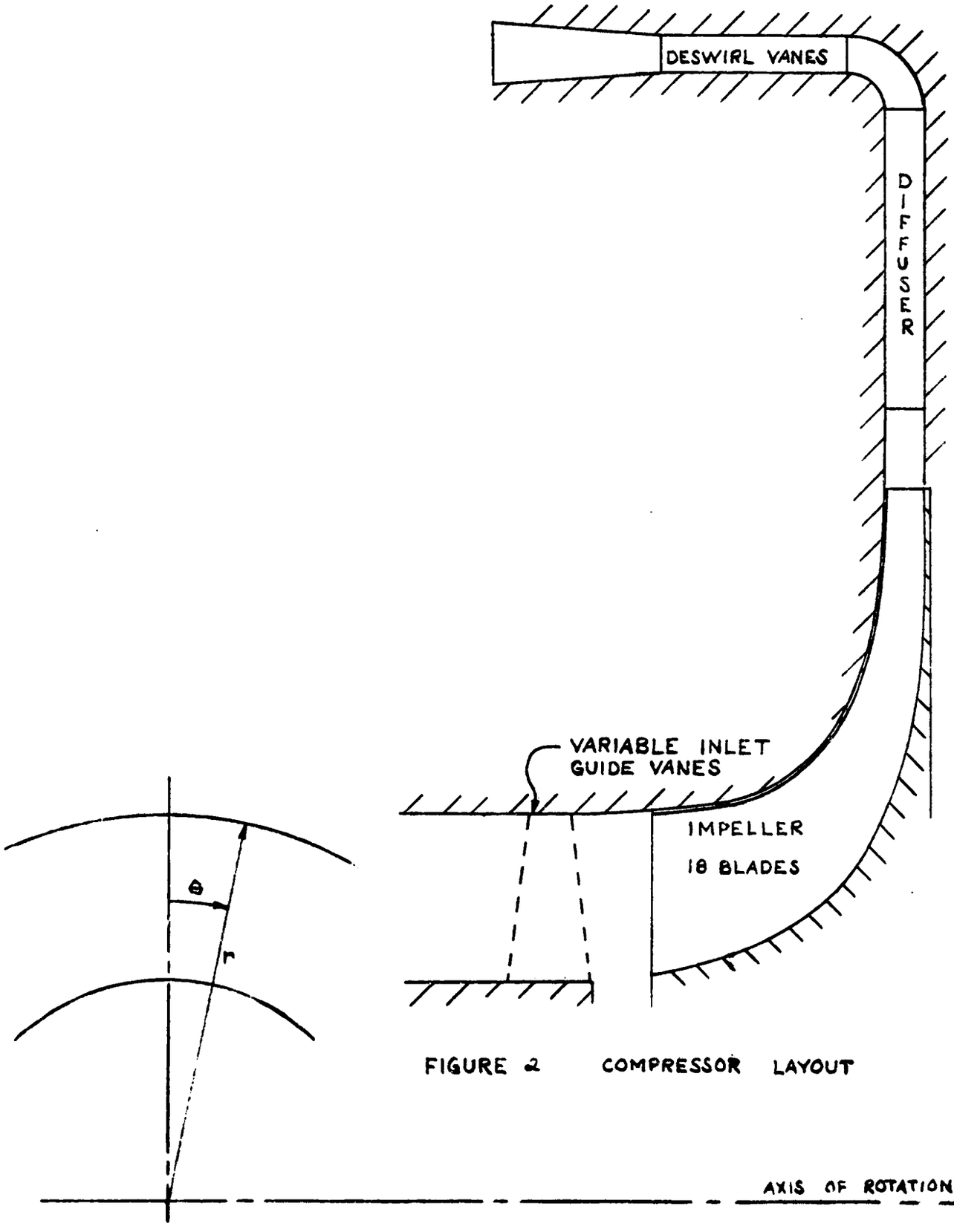


FIGURE 2 COMPRESSOR LAYOUT

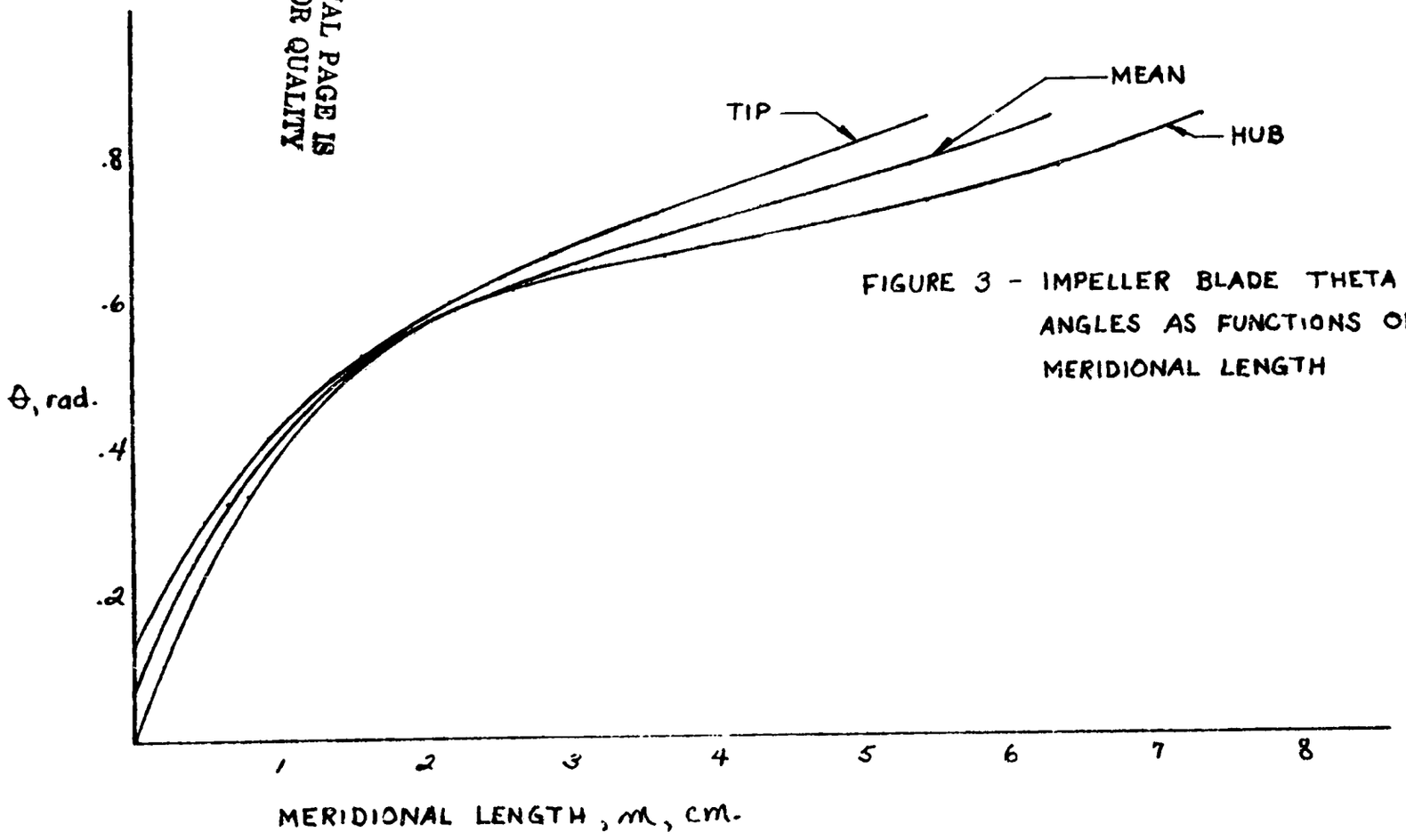


FIGURE 3 - IMPELLER BLADE THETA ANGLES AS FUNCTIONS OF MERIDIONAL LENGTH

FIGURE 4a - HUB SURFACE VELOCITIES AS FUNCTIONS OF MERIDIONAL LENGTH

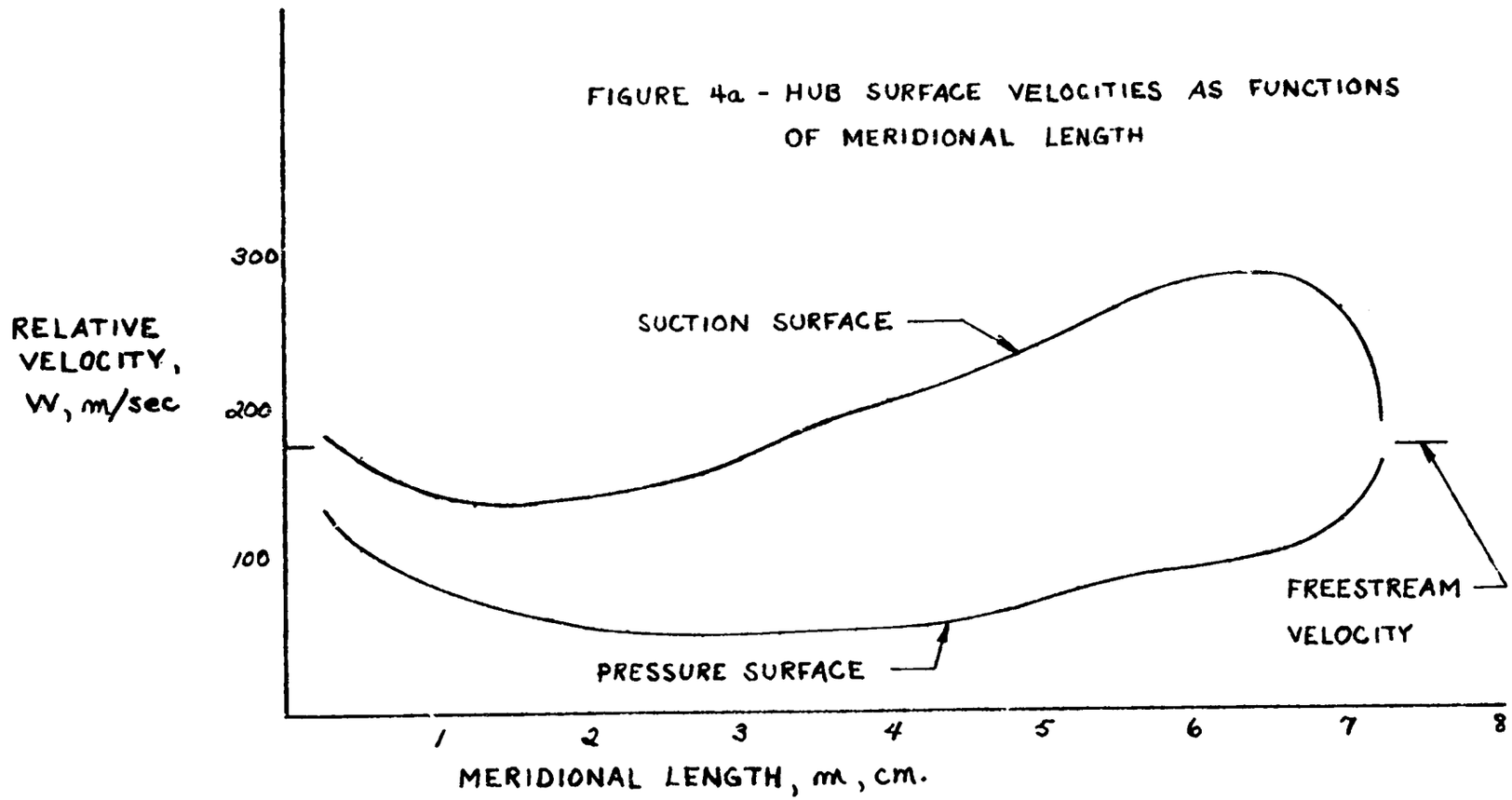

FIGURE 46 - MEAN STREAMLINE SURFACE VELOCITIES AS FUNCTIONS OF MERIDIONAL LENGTH

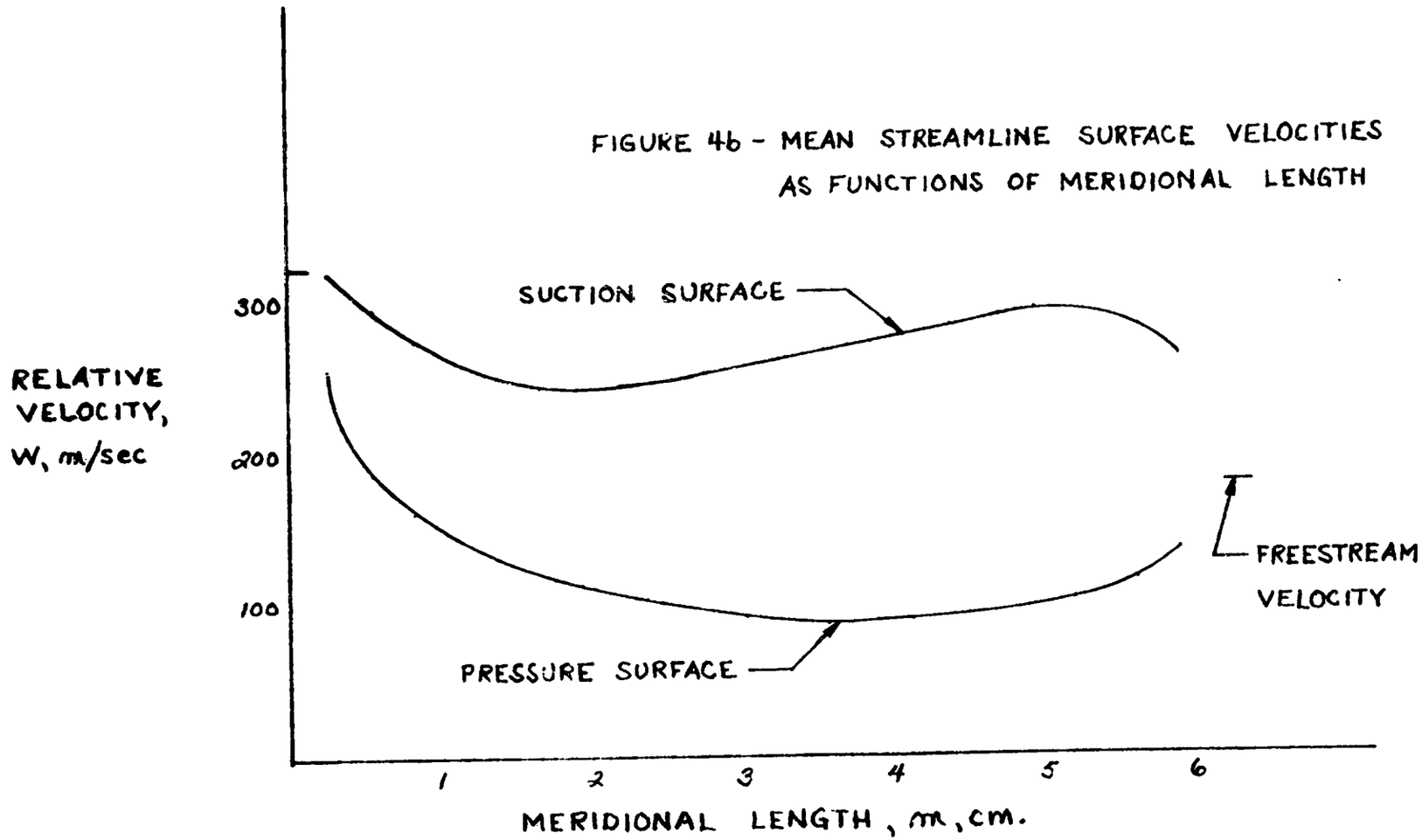

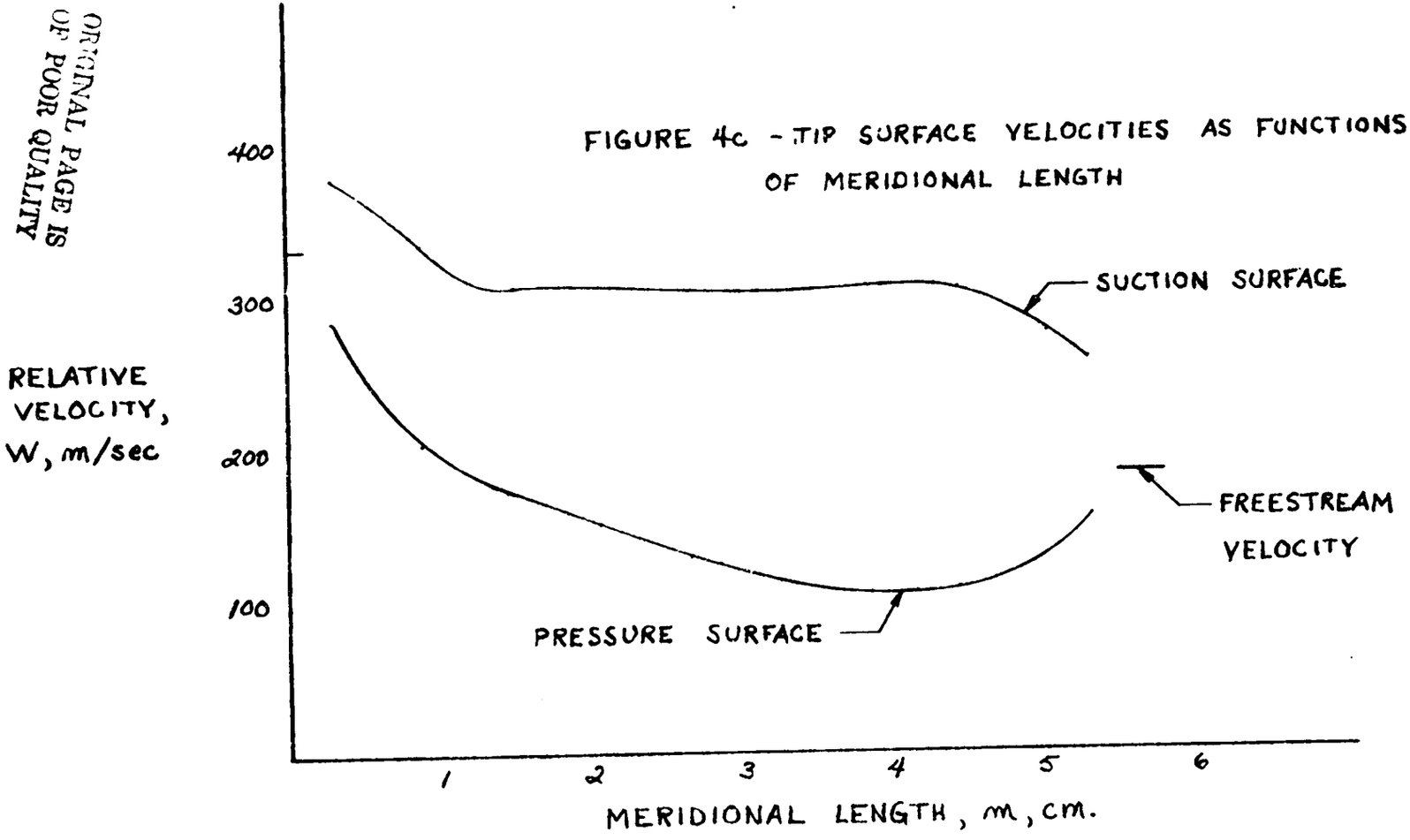


FIGURE 4c - TIP SURFACE VELOCITIES AS FUNCTIONS OF MERIDIONAL LENGTH

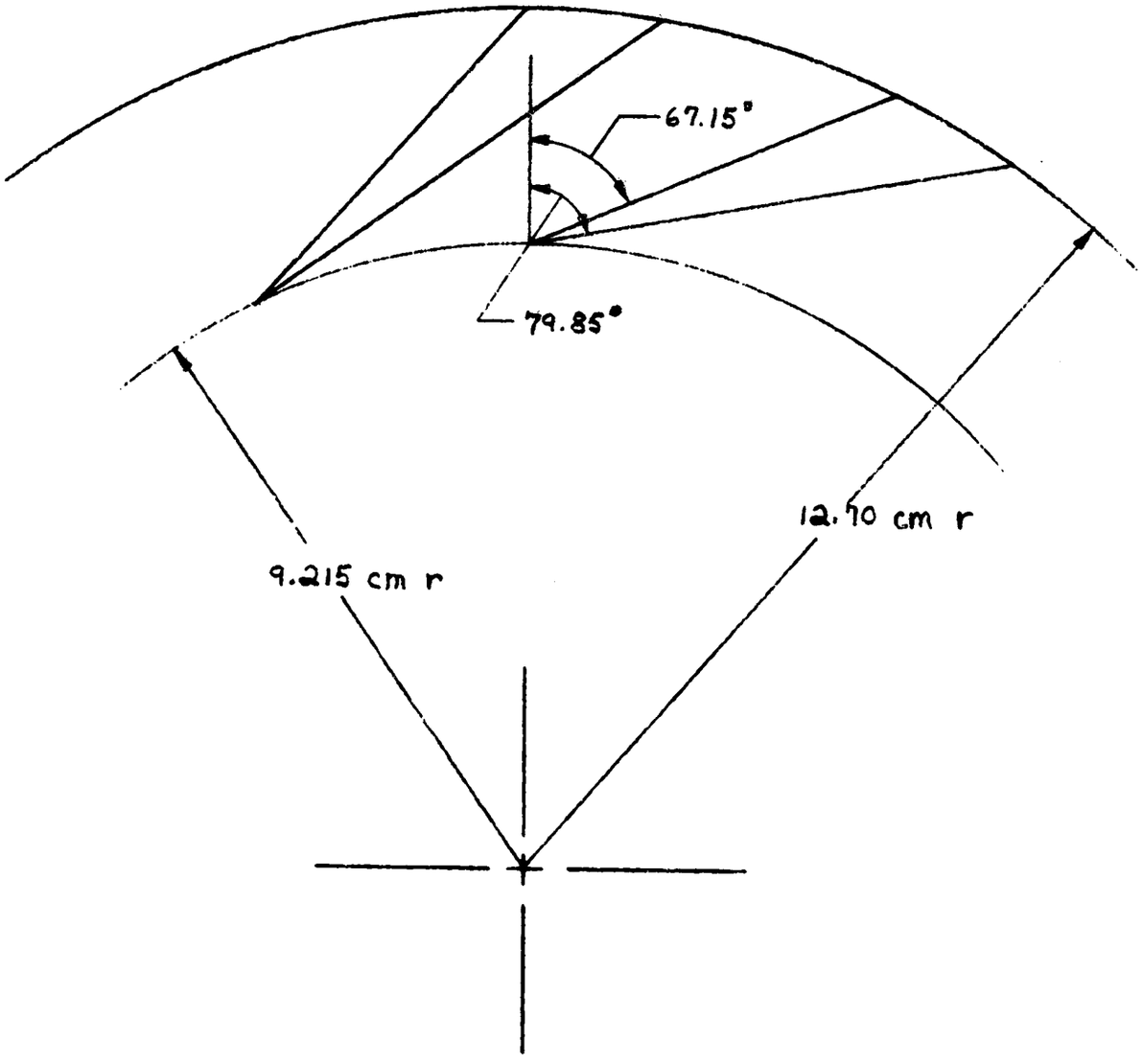


FIGURE 5 - CHANNEL DIFFUSER GEOMETRY (14 VANES)

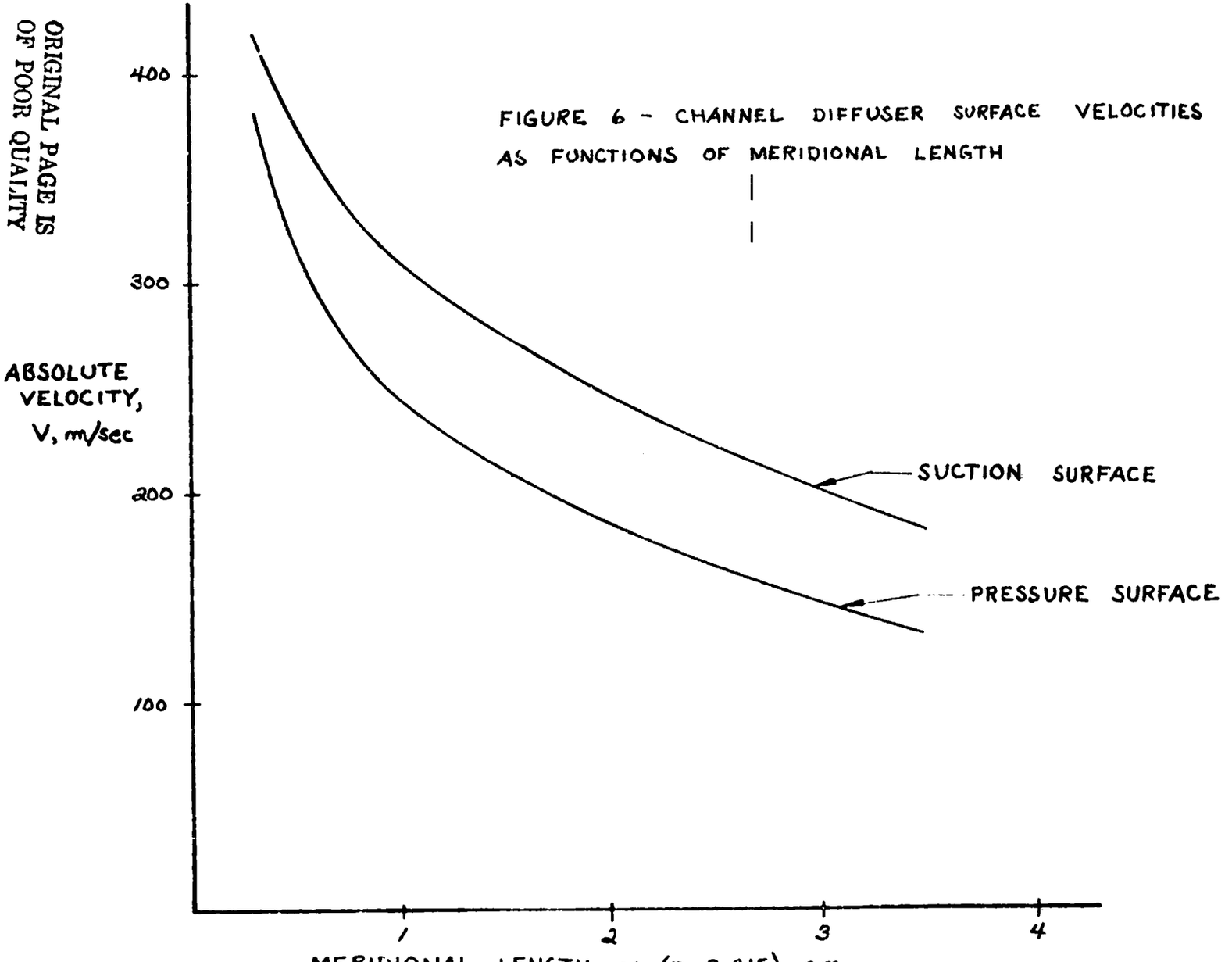


FIGURE 6 - CHANNEL DIFFUSER SURFACE VELOCITIES AS FUNCTIONS OF MERIDIONAL LENGTH

FIGURE 7 - TURNING DUCT WALL VELOCITIES AS FUNCTIONS OF MERIDIONAL LENGTH

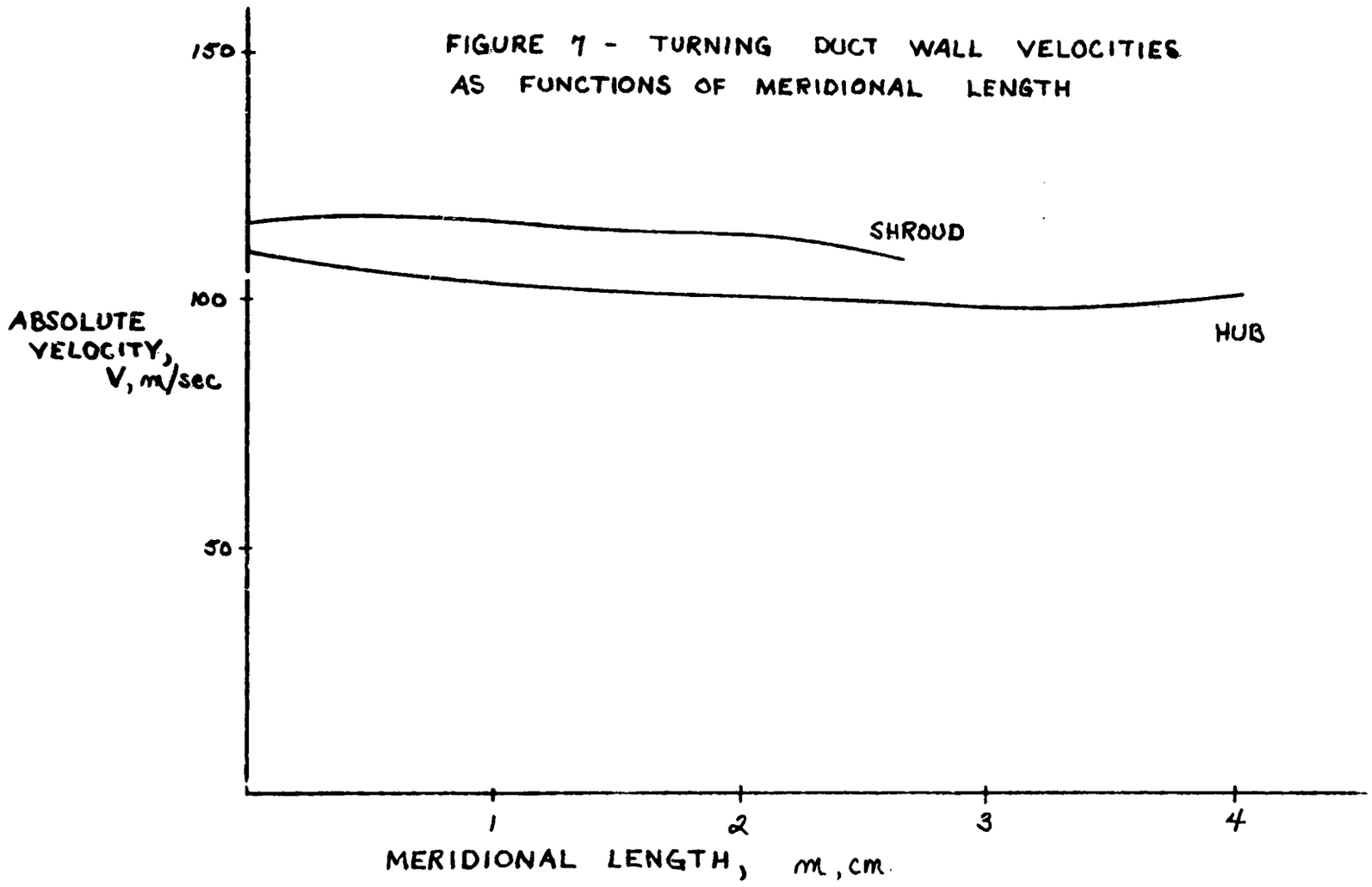

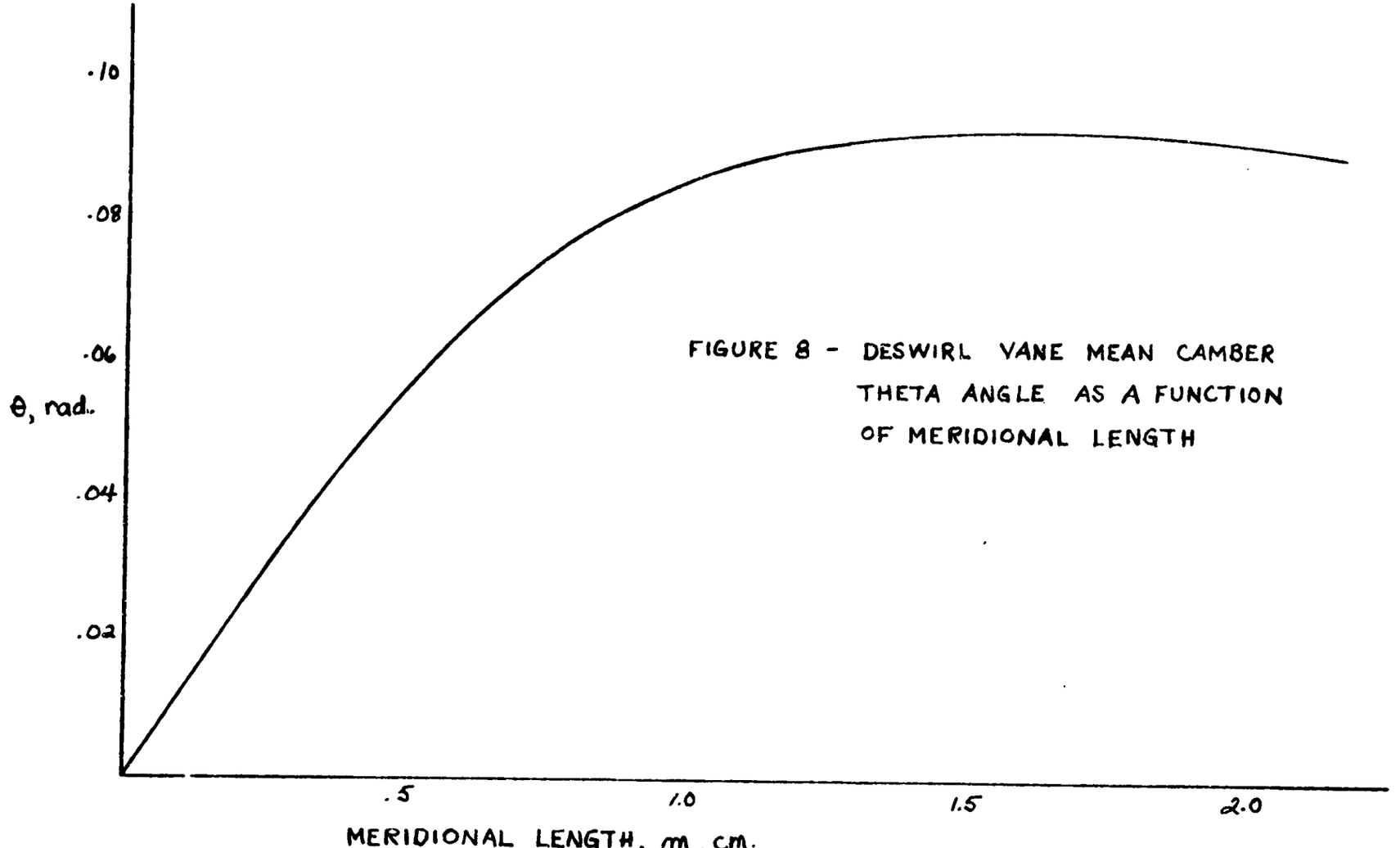


FIGURE 8 - DESWIRL VANE MEAN CAMBER THETA ANGLE AS A FUNCTION OF MERIDIONAL LENGTH

FIGURE 9 - DESWIRL VANE MEAN RADIUS SURFACE VELOCITIES AS FUNCTIONS OF MERIDIONAL LENGTH